

Ultra Nanoindentation Tester

//// Active top referencing (Patented Design)

The reference is removable and can be of different shapes (ball, pin, etc). The reference has its own piezo actuator and load sensor and applies a very small controlled (servo loop) load on the sample.

//// Thermal drift free

The head is constructed out of ZeroDur® glass and the electronics system has a drift rate of $\approx 1 \text{ ppm}/^\circ\text{C}$.

//// Highest load frame stiffness

Synthetic granite base platform, ZeroDur and the patented active top referencing.

//// Two independent depth and load sensors

Ultra high resolution capacitive sensors for True Depth and Load Control modes.

//// Ultra high resolution and very low noise floor

Depth resolution: 0.001 nm, noise floor $\approx 0.1 \text{ nm}$

Force resolution: 0.01 μN , noise floor $\approx 0.5 \mu\text{N}$

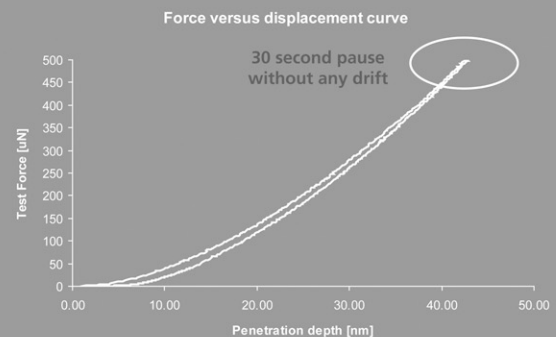
//// Perfect positional synchronization

The Ultra Nanoindentation Tester is perfectly "positionally synchronized" with a high quality optical video microscope and/or an optional Atomic Force Microscope (AFM).

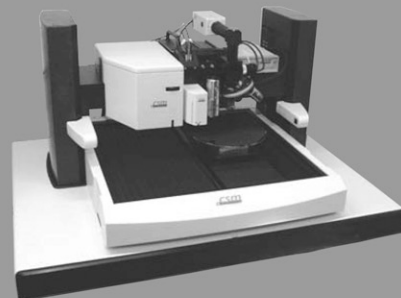
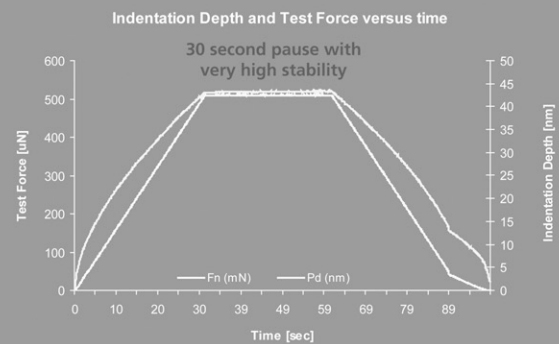
The combination of the Ultra Nanoindentation Tester head, the optical microscope and the AFM objective provides great flexibility and ease-of-use, as well as accurate three-dimensional imaging at the nanometer scale.

//// Compliant to ISO 14577 and ASTM E2546

CSM Instruments produces instruments and measurements that conform exactly to ISO and ASTM standards



//// Very high stability, no thermal drift



To learn more about the CSM Ultra Nanoindentation Tester, visit us on the web at www.csm-instruments.com

Novel ultra nanoindentation method with extremely low thermal drift: Principle and experimental results

J. Nohava

CSM Instruments SA, Rue de la Gare 4, Peseux CH-2034, Switzerland

N.X. Randall^{a)}

CSM Instruments Inc., Needham, Massachusetts 02494

N. Conté

CSM Instruments SA, Rue de la Gare 4, Peseux CH-2034, Switzerland

(Received 24 July 2008; accepted 20 October 2008)

Despite active development over the past 15 years, contemporary nanoindentation methods still suffer serious drawbacks, particularly long thermal stabilization and thermal drift, which limit the duration of the measurements to only a short period of time. The presented work introduces a novel ultra nanoindentation method that uses loads from the μN range up to 50 mN, is capable of performing long-term stable measurements, and has negligible frame compliance. The method is based on a novel patented design, which uses an active top referencing system. Several materials were used to demonstrate the performance of the method. The measurements with hold at maximum load confirm extremely low levels of instrument thermal drift. The presented Ultra Nanoindentation Tester opens new possibilities for testing thin films and long-term testing, including creep of polymers at high resolution without the need of long thermal stabilization.

I. INTRODUCTION

Recent advances in materials research have motivated the development of nanoindentation instruments using extremely low loads and depths. Several such instruments have been proposed to answer this need. These instruments allow the use of loads from several tens of μN up to several mN and can measure depth within a few nm up to a few hundreds of nm. Once such low loads and penetration depths are applied and measured, appropriate working conditions must be ensured. Nanoindentation machines are generally placed in a soundproof enclosure on an antivibration table to eliminate the transfer of vibrations and noise to the displacement and load signals. Of great importance is the thermal stability of the environment: the temperature variation should not exceed $0.5\text{ }^\circ\text{C/h}$. This criterion is crucial for nearly all presently commercially available instruments as they all suffer, to some degree, the problem of thermal drift.^{1–3} The phenomenon of thermal drift is well known in the nanoindentation field and significantly limits the use of such instruments for long-term measurements. Although the term “thermal drift” has never been properly defined, it is widely understood as “the change in the indentation depth when the force on the indenter is maintained constant and the

material does not exhibit time-dependent mechanical-properties.” Materials that do not exhibit time-dependent properties do not change their deformation in time while constant load is applied. The thermal drift adds an error value to the displacement signal that must be subsequently removed to extract the true indentation depth. To minimize the problem of thermal drift, two main approaches have generally been used.

(i) Maintaining the system and sample in an enclosure until the temperature becomes sufficiently stabilized for a measurement to be made.

(ii) Performing the indentation cycle very quickly, within a few seconds.

In both cases the thermal drift is minimized, but not removed, and subsequent steps are always required to take this into account. Many systems require a long hold of the indenter (in air) while the displacement signal is monitored, after which a software model is used to estimate the instrument drift rate. This approach has many disadvantages; the hold takes a long time (typically minutes or even hours), holding the indenter in the air is not representative of drift during the subsequent test, and the measured drift rate is nearly always assumed to be constant when it is not.

Although placing the instrument in a thermally insulating enclosure has the advantage of using the same enclosure as an antivibration shield, typical stabilization times can be up to several hours before any

^{a)}Address all correspondence to this author.

e-mail: nra@csm-instruments.com

DOI: 10.1557/JMR.2009.0127

measurement can be started. Other systems combine both methods, i.e., thermally insulated and antivibration enclosure with the measurements performed at a rapid rate. Results obtained under such conditions have been shown to be satisfactory, because the error in the displacement signal due to thermal drift of the whole system in such a short time is negligible.⁴ However, fast measurements do not conform to ISO 14577 and ASTM E 2546-07 nanoindentation standards^{5,6} that require 30 s for loading and 30 s for unloading. Furthermore, both approaches are insufficient for creep or long-term measurements. Another problem that must be dealt with is the compliance of the frame. During the indentation load–unload cycle, the whole system is being deformed. Although the stiffness of the frame is usually high and the loads are very low, the deformation of the frame still affects the displacement measurement. This problem is partially solved in contemporary systems by introducing a parameter for frame stiffness, which is used for correction of displacement at a given load. However, this parameter does not take into account any localized compliance introduced from the sample itself.

CSM Instruments has been working for several years on development of an instrument that would successfully address the previously mentioned problems. The Nanoindentation Tester (NHT) developed and commercialized in 1997^{7–9} has been shown to greatly reduce the problem of thermal drift and frame compliance by the novel use of a passive top referencing system. This work introduces an ultra nanoindentation system, which takes the technology several steps further, resulting in a high resolution ultra nanoindentation instrument with active top referencing, which eliminates almost entirely the problem of frame compliance and thermal drift. Such substantial improvement has been achieved by the use of a unique principle of load and displacement measurements. So far all existing nanoindentation systems have been based on only one actuator and one sensor. The new ultra nanoindentation method uses two separated actuators and three separated sensors, which provide real measurements of depth and load, as well as a feedback loop that allows continuous and accurate control of the applied load.¹⁰ The components used in the measurement head are made of innovative materials with extremely low coefficient of thermal expansion (CTE), which results in extremely low thermal dilation. The use of such materials in combination with the active top referencing system and an automatic compensation using a symmetric mechanical design leads to excellent thermal stability of the measurements and almost zero thermal drift. Because the problem of thermal drift and frame compliance has been almost completely eliminated in the UNHT instrument, all measurements shown in this work are raw data without any software or hardware correction of thermal drift or frame compliance.

II. EXPERIMENTAL

A. Instrument setup

The nanoindentation instrument developed at CSM Instruments and commercially named “Ultra Nanoindentation Tester” (UNHT) can be mounted as a module on either of two platform configurations; the Open Platform (OPX), which allows a total of four modules, and the Compact Platform (CPX), which allows a total of three modules. The other additional modules are an integrated optical video microscope and a choice of Atomic Force Microscope (AFM), Nanoindentation Tester (NHT), Nano Scratch Tester (NST), Micro Scratch Tester (MST) and Microindentation Tester (MHT). In both configurations, all modules are positionally synchronized to each other via displacement tables, which can translate the sample in *X*, *Y*, and *Z* axes with a repositioning resolution up to 0.1 μm . Figure 1 shows a typical instrumental setup on an OPX. The UNHT module was mounted with a Berkovich indenter for all tests, although any other type of indenter can be used, such as cube corner, spheroconical, or flat punch. The exchange of the indenter is easy and can be performed by the user. The whole assembly is placed on an antivibration table in a soundproof enclosure.

1. The UNHT principle

The principle of the UNHT is based on the idea of using two independent vertical axes: one axis is dedicated to the indentation measurement itself and one axis is used for active top referencing (see Fig. 2). Each axis has its own actuator and its own displacement and load sensors. For both axes, the displacement is applied via a piezo actuator and a spring of known stiffness. The stiffness of the spring is calibrated using a certified force



FIG. 1. The UNHT mounted on the OPX platform. The configuration includes (1) Ultra Nanoindentation measurement head, (2) Nanoindentation measurement head, (3) AFM microscope, and (4) optical microscope with camera.

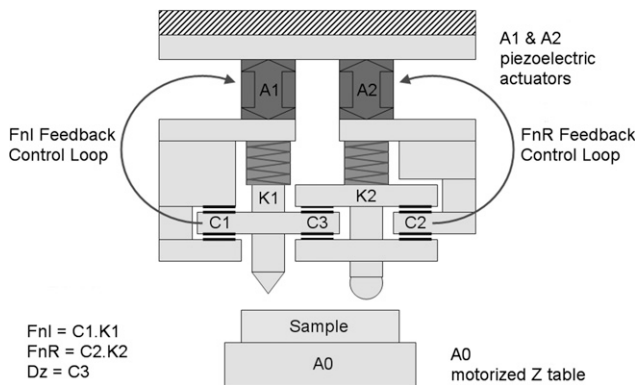


FIG. 2. Two-axis UNHT principle: **A0** represents the displacement of the motorized **Z** table, **A1** and **A2** are the piezo actuators used for the application of both forces: the active reference force, **F_{nR}**, and the normal force of the indenter, **F_{nI}**. **K1**, and **K2** represent the springs used in the system for application of the forces involved. The indentation depth of the indenter tip, **Dz**, is directly measured with the differential capacitive sensor **C3**. The software combined with the electronic control unit provides the appropriate feedback loop control of both forces.

gauge and a displacement actuator. The precision of calibration is in the range of 0.03% of their total range. The displacement of the spring is measured via capacitive sensor; using the stiffness of the spring the load on the indenter is calculated. The reference is usually of a spherical geometry, typically with a diameter of 3 mm and is placed on the right side of the indenter (front view). The distance between the indenter and the reference is 3 mm. Both indenter and reference have a total vertical travel of ~100 μm, and their respective initial position can be adjusted by the user. This means that samples with a height difference of up to 100 μm over 3 mm (3.3% tilt) can be tested. Samples whose dimensions are smaller than 3 mm can equally be tested when placed in a specially designed sample-holder on which the reference is positioned.

The load on the reference is calculated the same way as for the indenter, i.e., using a piezo actuator, spring with known stiffness, and capacitive sensor. The system (schematically shown in Fig. 2) can be better understood by considering it as two nanoindentation systems, which are intimately linked: one responsible for active top referencing of the sample surface and the other for performing the indentation. The load on both indenter and reference can therefore be independently controlled.

The key advantages of this novel design are as follows:

- (i) Active top referencing with very low applied loads, which are maintained constant during the entire indentation process by a dedicated feedback servo loop.
- (ii) Three capacitive sensors (**C1**, **C2**, **C3**) for direct measurement of depth and load where **C1** measures the

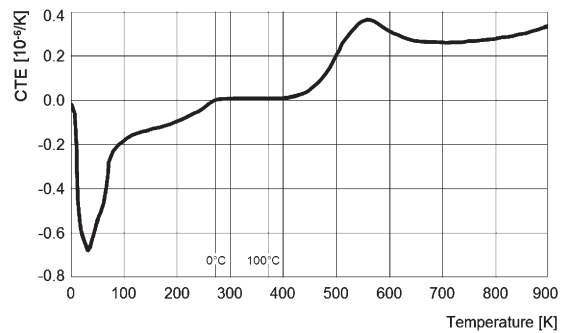


FIG. 3. Coefficient of thermal expansion of the Zerodur material used in the construction of the UNHT head (reprinted from Schott AG, Germany). Note the quasi-zero thermal expansion coefficient over the temperature range 0–100 °C.

indentation axis, **C2** measures load on the reference axis, and **C3** measures the displacement of the indentation axis relative to the reference axis.

(iii) Two piezo actuators (**A1**, **A2**) for a compact and rigid design without temperature effect. Two force sensors are used for two independent feedback loop controls: one for the load applied by the reference and one for the load applied by the indenter.

Superior thermal stability of the whole assembly is achieved with the use of Zerodur material (Schott AG, Mainz, Germany) with a CTE as low as 0.1×10^{-6} K in the range of 0 to 100 °C, as shown in Fig. 3. This means that the system has quasi-zero thermal expansion or contraction over the standard operating temperature of the instrument.

2. Instrument frame compliance

An independent control of the reference axis allows the elimination of the effects of small displacements of the surface and/or instrument caused by deformation of the frame and the sample.¹¹ During nanometer-scale measurements, such displacements are often in the same range as the measured quantities and can negatively influence the results. In the case of the UNHT, the reference is maintained in contact with the sample surface at a given load during the whole indentation cycle and therefore follows all movements of the sample. The displacement sensors in the UNHT head assembly are therefore “floating” on the sample surface and the displacement signal is not influenced by deformation of either the frame or the sample. As a result, this design reduces to a large extent the effect of the frame and almost completely eliminates the necessity of correction of the frame compliance. In addition, the load applied by the reference can be adjusted to suit the type of material being measured.

3. Penetration of the reference

The penetration of the reference into the tested material, even when using loads as low as 10 μN, is not

negligible when the maximum penetration depth during indentation is in the range of tens of nanometers. However, this does not present any influence on materials that do not exhibit creep, and only a minor influence on materials that creep. Once the defined load is applied on the reference touching the surface, it will penetrate into the material because of pressure applied to the material via the spherical reference. This penetration depth depends on the elastic–plastic behavior of the material. However, the penetration depth will remain constant as the load on the reference is maintained constant throughout the whole indenter approach and the indentation itself. The indentation depth of the indenter is measured relative to the reference whose position is not changing because the load on the reference is maintained constant. Therefore, even though the reference can be impressed several nanometers into the material, it will not influence the indenter displacement measurement.

On a material with creep, the problem is more complicated because the reference keeps penetrating even after the defined load was fully applied on it. However, this issue has been dealt with in three complimentary ways: use of special reference in the form of a spherical cap with large radius, low load on the reference, and longer time for indenter approach. The first two cases are not an issue for the UNHT system since the large radius reference can be installed by default and the thermal stabilization period before the indenter approach (included in the indentation procedure) leads to stabilization of the depth change (see Fig. 8). The load on the reference can be calculated so that the pressure on the material is as low as possible. As a result, when the indentation starts, the penetration depth of the reference should already be stable or the change negligible and the equilibrium state reached for materials without creep.

4. Instrument thermal drift

Small temperature changes cause dimensional variations of the sample and the frame that induce drift in the displacement measurements. This problem is critical for nanoindentation systems without any reference of the surface.^{11,12} In the case of the UNHT, the solution to this problem was found in the use of piezoelectric actuators with the active referencing system whose components are made of materials with extremely low coefficient of thermal expansion. Such design of the instrument minimizes the effects of thermal drift, i.e., thermal dilatation of the sample and the frame. As the displacement of the indenter is measured with respect to the reference, which is “floating” on the sample surface, all thermal dilatation of the sample and the frame are simply disregarded. Although in other nanoindentation systems the thermal drift correction must

be applied to the displacement signal, the UNHT works directly with the data without any hardware or software corrections.

5. Surface approach and detection

The entire indentation process can be divided into several phases: approach of indenter to the surface, contact of the indenter with the surface, the indentation cycle itself (i.e., controlled loading and unloading), and subsequent retraction of the indenter from the surface. Several parameters can be set to optimize the approach process and the contact detection. The speed of the indenter, during surface approach, can be set from 200 nm/min for small loads and hard materials up to 4000 nm/min for soft materials and/or high loads.

The contact of the indenter with the surface is detected by the software as a change in the contact stiffness. This criterion can be adjusted by the user to suit the material tested. The contact point, i.e., the position where the indenter touches the sample surface, is chosen by the software as the first point where the force signal starts to increase from its zero value (the indenter is in the air and there is no load applied on the indenter) during indenter approach. To successfully detect even a slight change in force in indentation of soft materials, the slope of a linear fit of the preceding and succeeding 30 data points are calculated for each data point. Once the difference in the two slopes is greater than 30% the data point is taken as a contact point. The contact point detected by the software can also be adjusted manually by the user, but generally the adjustment of contact point leads to variation in the results of less than 1% or 2%. The contact point is then used to calculate the depth of contact, from which the indentation hardness and modulus values can be calculated.¹³

6. Force controlled and depth controlled indentation

In most applications indentation is done in a force controlled mode while the resultant indentation depth is recorded. This is common because most contemporary nanoindentation systems can only be operated in a force controlled mode. For many materials, particularly engineering metals and ceramics, this mode has been satisfactory for extracting accurate mechanical properties. However, with extended use of nanoindentation for investigating soft viscoelastic polymers, other modes have gained attention because mechanical properties of these materials are deformation rate dependent. The presented UNHT uses three force controlled and two indentation depth controlled modes for indentation. The force controlled modes are linear loading, quadratic loading, and constant strain loading. Linear loading is the most widely used—force is increased and decreased

in a linear manner. Quadratic loading is used to straighten the penetration depth versus time curve. Constant strain loading the mode is based on the method described in Ref. 14 and is used mainly for testing of polymers because it controls the load so that strain rate is maintained constant.

The UNHT disposes of two indentation depth controlled modes. In the maximum indentation depth mode the force is increased at a given rate until the specified indentation depth is reached. The full depth controlled mode allows the user to set the displacement rate, and the force is then adjusted automatically to follow this rate up to the preselected maximum indentation depth value. The full depth controlled mode allows any measurement to be performed where constant indentation depth rate is required, such as for the assessment of toughness in thin coatings.¹⁵

7. UNHT specifications

The UNHT can be operated over two user defined load and depth ranges; the fine range provides a maximum applied load of 10 mN with a resolution of 1 nN, the standard range provides a maximum applied load of 50 mN (optionally 100 mN). The respective displacement range and resolution is 10 μm and 0.0003 nm for the former and 100 μm and 0.002 nm for the latter. The loading rate can be set from 0 mN/min up to 1000 mN/min. The typical approach speed is 1000 nm/min. The real noise on both force and displacement signals was evaluated during measurements with pause at maximum force on fused silica. The noise on the force both during indenter approach and during the pause on fused silica in standard laboratory conditions was less than 0.3 μN . The noise on the displacement signal during 120 s pause at maximum force was 0.2 nm.

B. Experimental procedure

1. Samples

The samples used for measurements were selected so that hard, soft plastic, and elastic material types would be represented to confirm the applicability of the UNHT system to all classes of materials. All tested samples exhibited flat, mirrorlike surfaces so that the influence of surface roughness would be minimized, even for indentation tests at low penetration depths. Except for the fused silica, which was placed and held directly in the vice of the UNHT sample holder, all other samples were attached using Loctite cyanoacrylate adhesive (Henkel AG, Pratteln, Switzerland) on an aluminum cube and then fixed in the vice. The surface of the tested samples was cleaned by oil-free compressed air dust cleaner; no other cleaning methods were used.

2. Fused silica

A polished fused silica cylinder (25 mm diameter, 5 mm thickness) was used because it is a reference material in nanoindentation. Mechanical properties of fused silica are known to be time independent at room temperature, and the material is suitable for measurements of instrument thermal drift. Therefore, an important part of the measurements was done on this material to demonstrate the low values of thermal drift and frame compliance.

3. Polymers

The measurements of mechanical properties of polymers were performed on three bulk samples: poly(methyl methacrylate) (PMMA), poly(vinyl chloride) (PVC), and polycarbonate (PC). The samples in dimensions of $\sim 25 \text{ mm} \times 25 \text{ mm}$ were cut from commercially available sheets of 2.5 mm thickness.

4. Thin coatings

The ability of the instrument to test thin coatings was demonstrated on four samples: diamondlike carbon (DLC), SiO_x , Cr-doped C coatings, and commercial polymeric paint coating. The thicknesses of the coatings and substrates were respectively 1 μm for the DLC coating on steel, 500 nm for the SiO_x coating on Si wafer, 50 nm for the Cr-doped C coating on Si wafer, and 40 μm for the polymeric paint on 2-mm-thick plastic sheet.

5. Main indentation parameters

All measurements were performed using the CSM Instruments UNHT with a Berkovich indenter. The shape function of the indenter was determined by a matrix of indentations at various loads on fused silica. The indentations were performed according to ISO/ASTM standards^{5,6}: 30 s for loading and 30 s for unloading. Loading and unloading was done in force controlled mode with linear load increase. The maximum force varied from 20 μN to 10 mN. The contact load, i.e., the load threshold at which the indentation starts, was set to 5, 10, 15, and 50 μN depending on the maximum load used. The contact point (the point where the indenter first touches the sample surface) was determined according to ISO/ASTM standards as the first point on the loading–unloading curve where the load started to increase. The measurements of stability were done with a pause of 60, 120, or 300 s at the maximum indentation load. The creep on polymers was calculated as the difference between the displacement at the beginning of the pause and the displacement at the end of the pause divided by the displacement at the beginning of the pause. The calculations of elastic modulus and hardness were based on modified Oliver and Pharr theory.¹³

III. RESULTS AND DISCUSSION

A. Fused silica measurements

Fused silica is often used as a reference material for nanoindentation. The verification of the precision, frame compliance, and thermal drift was therefore done on this material. Figure 4 shows typical load-penetration depth graphs with maximum indentation loads of 100 and 1000 μN . The contact load was set to 10 μN for the 100 μN and 30 μN for the 1000 μN load. There were 10 measurements performed at each maximum indentation load. The elastic modulus calculated for the 100 μN load was $72.3 \pm 1.7 \text{ GPa}$ and $72.2 \pm 1.8 \text{ GPa}$ for the 1000 μN load. These values are in agreement with the specifications of the fused silica sample ($72.0 \pm 2.0 \text{ GPa}$), as provided by the manufacturer (Saint Gobain Glass AG, Switzerland).

1. Instrument frame compliance

The frame compliance, i.e., deformation of the frame due to indentation load, has been investigated by indentations on fused silica. The indentations were done at different maximum loads so that a set of (total compliance, F_{max}) data pairs was obtained. Total compliance or C was calculated from the unloading part of the loading–unloading curve. F_{max} is the maximum applied load during the indentation.^{13,16} The following equation puts in relation the total compliance C , sample compliance C_s , and frame compliance C_f :

$$C = C_s + C_f \quad , \quad (1)$$

where C_f (frame compliance) is considered as a constant. Using the formula for calculation of reduced modulus E_r the compliance of the sample C_s can be rewritten as a function of projected area of contact A_p . A_p can be further written as hardness F_{max} divided by hardness H_{IT} .^{16,17} Assuming that hardness of fused silica is constant yields $A_p \propto F_{\text{max}}$. According to ISO 14577 standard⁶ the sample compliance can then be expressed as a function of $1/F_{\text{max}}$. The total compliance C is obtained directly from the loading–unloading curve, if plotted against $1/F_{\text{max}}$ it should lead to a straight line.

The intersection of this line with the Y axis gives the value of frame compliance C_f . The result of such a fit is shown in Fig. 5 with the linear equation for the linear fit on the graph. The intersection of the linear fit is 0.002, i.e., the frame compliance is 0.002 nm/mN. This is two orders of magnitude less than that of some other instruments¹⁸ and even CSM Instruments higher load NHT whose frame compliance is 0.2 nm/mN. In the CSM Instruments indentation software the frame compliance is set to zero and no frame compliance correction is done on the experimental data. Although one may argue that the calculated frame compliance has a non-zero value, a large number of verification experiments at various loads has led to the conclusion that even if the frame compliance would be set to the calculated value of 0.002 nm/mN, its effect would be hidden by other factors that result in what is called experimental error. In other words, the effect of the frame compliance in the case of the UNHT is so small that it can be simply disregarded among other common sources of error.

Obviously the use of active referencing leads to practical elimination of frame compliance. In contrast with systems without reference, the frame compliance does not have to be corrected and raw indentation data can be used for calculation of mechanical properties of the sample.

2. Instrument thermal drift verification

The phenomenon of thermal drift, one of the major drawbacks of many indentation instruments, has been studied on the UNHT for two different cases: the drift of the force on the indenter during approach of the indenter to the sample surface and drift of the displacement signal during pause at maximum indentation force.

The stability of force during approach of the indenter to the surface is crucial for correct detection of the contact of the indenter with the sample surface. If the force signal drifts too much or if its noise is too high then a “false” contact may be detected. The concept of the UNHT ensures that the drift of the force is small, 0.1 $\mu\text{N}/\text{min}$ (see Fig. 6).

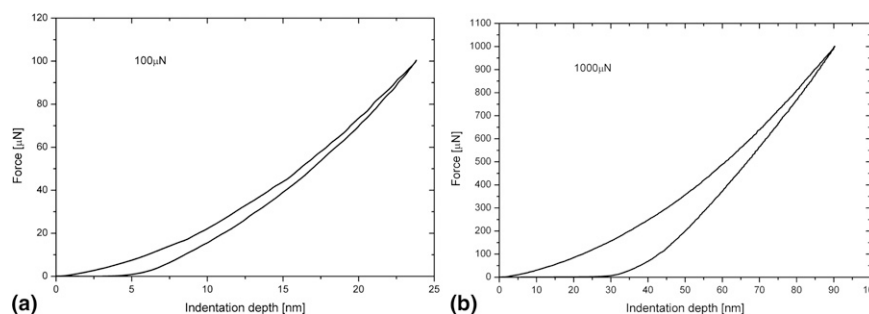


FIG. 4. Fused silica measurements at (a) 100° μN and (b) 1000° μN .

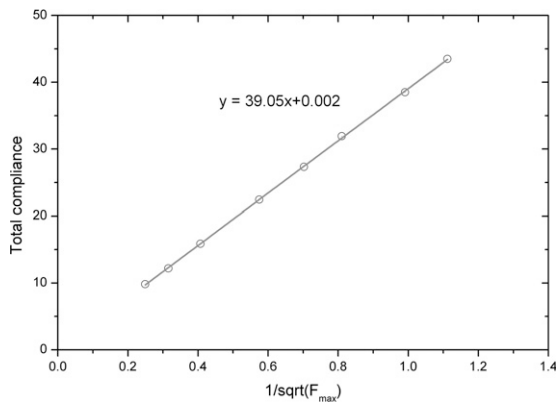


FIG. 5. Graphic determination of frame compliance from indentations on fused silica at various maximum indentation forces (F_{max}). The constant of 0.002 in the linear fit corresponds to frame compliance in nm/mN.

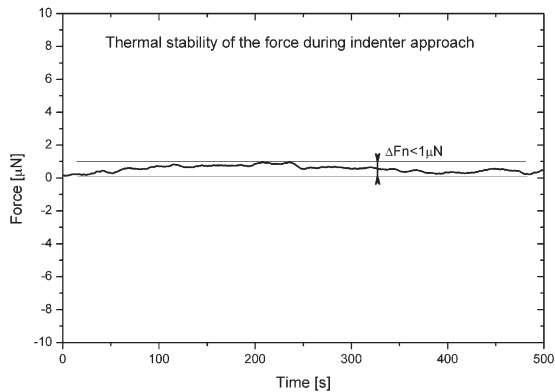


FIG. 6. Thermal stability of the force signal during 500 s approach of the indenter to the sample surface before the indentation. As the indenter is in the air and the force is therefore not controlled, it should be as close to zero as possible.

The stability of the displacement signal was measured during a pause when indenting fused silica. The measurements were performed with pause of 300 s at the maximum load. The maximum load varied from 50 μN to 1 mN; in all measurements the maximum load was reached in 30 s. Results obtained on fused silica with 1 mN load showed that the average drift was 0.87 nm (see Table I) with some measurements showing drift as low as 0.2 nm (Fig. 7). This is significantly lower than the thermal drift of other instruments¹⁹ where corrections of the thermal drift must be done numerically based on thermal drift values obtained either before or after the indentation.

Because the load on the reference is actively maintained constant during the whole duration of the indentation, the reference follows the surface of the sample. The true penetration depth of the indenter in the material is measured relative to the reference; hence, all movements of the sample that would otherwise affect the penetration

depth are disregarded with the UNHT. As seen in Fig. 7 and Table I the active top referencing system almost completely eliminates the thermal drift.

It should be noted that all presented measurements were performed in standard laboratory conditions and the resulting graphs are presented as is, i.e., without any software or hardware correction of thermal drift or frame compliance. The extremely low instrument thermal drift is therefore a direct result of the unique principle of the UNHT measurement head including top referencing system and components made from low CTE components.

B. Polymers

The low instrument thermal drift of the UNHT allows long-term measurements to be made that were impossible to perform on previous systems with high or unstable thermal drift.^{4,20} Among such measurements belong creep tests on polymers or other materials with time-dependent mechanical properties.

The measurements were performed on three bulk polymer samples. The maximum load of 1 mN was reached by linear loading in 30 s (according to the ISO 14577 standard).⁶ This maximum load was then maintained for a period of 120 s. All tested samples showed noticeable creep (see Fig. 8); the highest creep was observed for PMMA (57 nm), followed by PVC (46 nm),

TABLE I. Thermal drift of the UNHT during pause at different maximum test forces. Three to five tests were performed at each maximum test force. The results represent raw data without any software or hardware corrections.

Maximum test force (μN)	Duration of pause (s)	Drift (nm)
50	300	1.03 ± 0.51
100	300	0.76 ± 0.53
200	300	0.85 ± 0.29
1000	300	0.84 ± 0.46
Average drift (nm)		0.87 ± 0.47

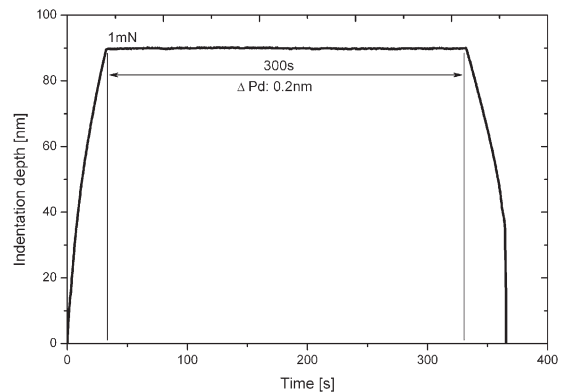


FIG. 7. Thermal drift evaluation: indentation on fused silica, 300 s pause at 1 mN load.

and PC with the lowest creep of 29 nm. The creep value (difference between the displacement at the end of the pause and the displacement at the beginning of the pause divided by the displacement at the beginning of the pause) is also shown on Fig. 8.

Obviously even after 120 s pause the penetration depth was still increasing. Because the maximum penetration depth is an important factor in hardness calculations, the time of creep will significantly affect the calculations of hardness of polymers. It is therefore important to establish a general rule for testing conditions on such materials so that all measurements are comparable. There can be two types of such criterion: a given duration of the pause, e.g., 60, 120, or 300 s, or time-dependent pause, or the pause is prolonged until the penetration depth increase rate falls under a predefined value (0.5% for example). Such criteria have previously been proposed by Feng et al.²⁰

The indentation tests on polymers also showed that the loading rate influences the level of creep during the pause. Higher loading rates led to higher creep, lower loading rates led to lower creep. This is easily understandable because during slower loading the sample has more time to accommodate the creep that would normally take place during the pause. Hence, the loading rate specifications must be included in the previously

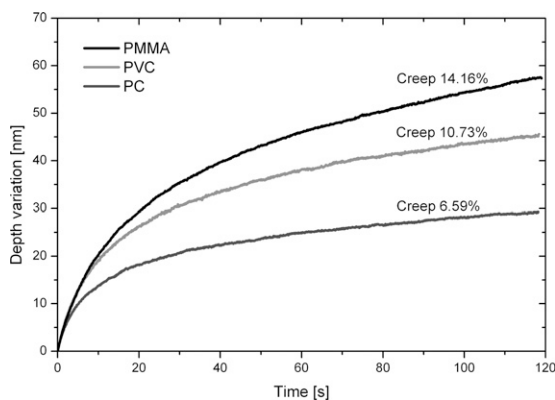


FIG. 8. Superposition of the depth-time graphs during the pause for the three tested polymers.

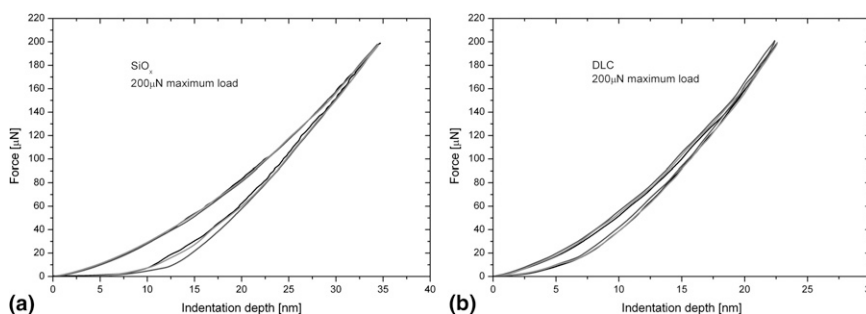


FIG. 9. Indentation graphs for the (a) SiO_x and (b) DLC samples.

suggested criteria or at least all measurements must be performed with the same loading rate.

C. Thin coatings

In the field of thin coatings, the “ten percent rule,” whereby the maximum penetration depth into the coating must not exceed 10% of the coating thickness, has been shown to give good mechanical properties for coatings independent of their substrates.^{11,21} In accordance with this rule, the tests on the DLC, SiO_x, and Cr-doped C coatings were performed at low loads to minimize the influence of the substrate on the results. In addition, tests on a 40-µm-thick polymer coating on polycarbonate substrate were performed to demonstrate the possibility of testing polymer coatings at low loads.

For the DLC and SiO_x coatings, the maximum applied load of 200 µN corresponded to a penetration depth of maximum 35 nm (coating thicknesses: 1 µm and 0.5 µm respectively). The resulting graphs from indentations with 200 µN maximum load are shown on Fig. 9. Three loading-unloading graphs are displayed, superimposed in each case, showing the high reproducibility for each sample and standard deviation (marked Error in Table II) well below 2% for both hardness and elastic modulus values (except the SiO_x sample, which showed standard deviation of ~4% for elastic modulus values).

According to preliminary tests of the Cr-doped C coating (whose thickness was only 50 nm), the maximum load was set to 65 µN giving a maximum penetration depth of 11 nm (see Fig. 10), which is ~20% of the thickness of the film. Lower loads were found to produce noisy results, although the measured values were similar. It is probable that the measured mechanical properties of the coating would be slightly affected by the substrate [Si(100) wafer].

The results obtained on the thin film samples confirm that the UHNT can be successfully used for indentations of coatings with a thickness less than 100 nm. The lowest penetration depths reached were ~11 nm and both load and displacement signals were not only very smooth but also highly repeatable.

TABLE II. Mechanical properties of the DLC, SiO_x, and Cr-doped C thin coatings. H_{IT} denotes indentation hardness, E_{IT} denotes indentation modulus.

Sample	H_{IT} (MPa)	E_{IT} (GPa)
DLC	9010 ± 80	95.89 ± 1.16
SiO _x	5862 ± 50	51.74 ± 1.98
Cr-doped C	15214 ± 177	155.39 ± 2.66

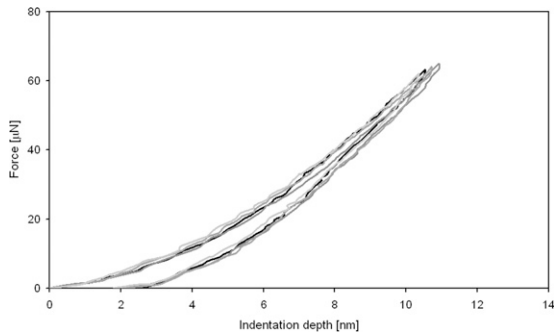


FIG. 10. Indentation graph with 65 µN maximum load for a Cr-doped C coating. Four loading–unloading curves performed under the same conditions are superimposed.

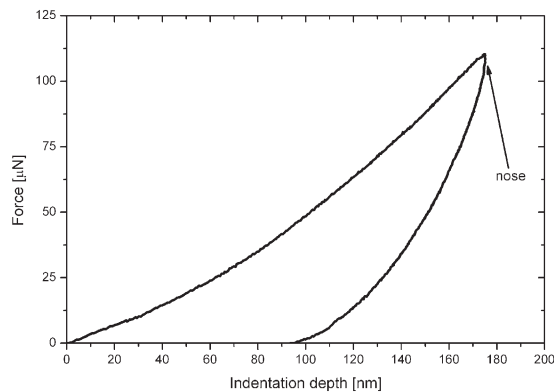


FIG. 11. Typical loading–unloading curve obtained on polymeric paint coating. Note the “nose” shape of the curve, which is a direct result of creep.

D. Polymeric coating

The tests performed on the polymeric paint coating (thickness of 40 µm) were aimed at demonstrating the applicability of the UNHT to measuring the surface mechanical properties of common polymer coatings. The measurement conditions were similar to those used for bulk polymer samples, i.e., linear loading/unloading, maximum load varied from 22 µN to 10 mN with 120 s pause at the maximum load. A typical indentation curve is shown on Fig. 11. Note the “nose” shape at the maximum load indicating time-dependent properties of the material: the penetration depth was increasing even when the applied load was decreasing. The creep properties of the tested polymer coating were confirmed in measurements with 120 s pause at 1 mN. The difference in penetration

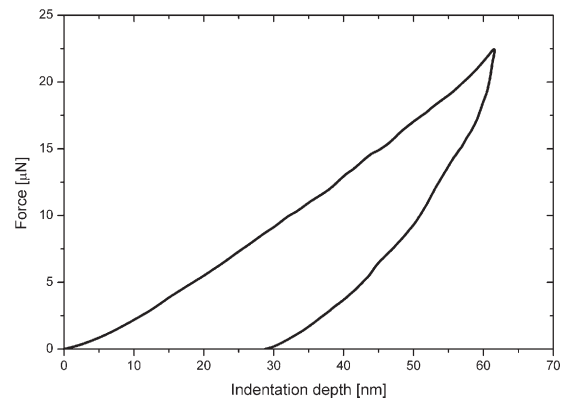


FIG. 12. An example of loading–unloading curve on the polymeric paint sample with maximum load of 22 µN.

depth after 120 s was 159 nm (creep of 25.63%), i.e., the highest out of all tested polymer samples.

The polymeric paint sample was also used to show the lowest limits of the load applied during indentation. Eight measurements were performed with a maximum load of 22 µN and contact load of 5 µN. The typical curves obtained from these measurements are shown on Fig. 12. The measured hardness and elastic modulus values were 315 ± 16 MPa and 3.71 ± 0.17 GPa, respectively. Applying low loads on polymers means that the indenter is operating closer to the elastic region: the nose shape of the curve, which is a result of the creep is much less pronounced on the 22 µN graph (see Fig. 12). Using spherical indenters, with large tip radii instead of a sharp Berkovich geometry, would lower the pressure in the material under the indenter and would therefore allow the mechanical behavior of polymers in compression to be studied. However, at penetration depths of a few nanometers or few tens of nanometers the UNHT is showing new phenomena, such as the tip defect of the indenter. Although some indenter suppliers do specify radius of the tip (typically 50–100 nm for Berkovich), the exact spherical form of the apex is not precisely defined. The calibration of the indenter area function at low penetration depths therefore becomes extremely important.

IV. CONCLUSIONS

It has been shown that the new UNHT allows the measurement of mechanical properties of various types of materials with extremely low-load indentations. The presented method has been tested on several types of materials and the results confirm the main advantages of the unique UNHT concept: extremely low thermal drift and negligible frame compliance. Such excellent performance has been achieved thanks to the active top referencing and use of material with low coefficient of thermal expansion in the construction of the measurement head. Indentations with a maximum depth

of 12 nm and load of 22 μN , according to ISO 14577 standard,⁶ have been performed. The precision and repeatability of the presented measurements confirm the applicability of the UNHT for thin coatings as well as for advanced materials where small-volume measurements are required. The absence of thermal drift allows the measurement of creep of both bulk polymer and thin polymer coatings with a several minute pause at maximum load. We strongly believe that this new instrument will prove itself in many fields, which require stable, precise, and long-term measurements at low loads and/or penetration depths. The additional benefits of a fast approach and no need for lengthy drift correction will also make this instrument very useful for making large matrices of indentations in relatively short time periods.

ACKNOWLEDGMENTS

The authors thank Richard Consiglio and Bertrand Bellaton of CSM Instruments for useful discussions in preparing this work.

REFERENCES

1. N. Schwarzer, T. Chudoba, and F. Richter: Investigation of ultra thin coatings using nanoindentation. *Surf. Coat. Technol.* **200**, 5566 (2006).
2. A.C. Fischer-Cripps: *The IBIS Handbook of Nanoindentation* (Fischer-Cripps Laboratories Pty Ltd., Australia, 2005), p. 60.
3. R. Zhang and H. Ma: Nano-mechanical properties and nano-tribological behaviors of nitrogen-doped diamond-like carbon (DLC) coatings. *J. Mater. Sci.* **41**, 1705 (2006).
4. T. Chudoba and F. Richter: Investigation of creep behaviour under load during indentation experiments and its influence on hardness and modulus results. *Surf. Coat. Technol.* **148**, 191 (2001).
5. ASTM E 2546-07: *Standard practice for instrumented indentation testing*.
6. ISO 14577: *Metallic materials—Instrumented indentation test for hardness and material parameters*.
7. N.X. Randall, R. Christoph, S. Droz, and C. Julia-Schmutz: Localized micro-hardness measurements with a combined scanning force microscope/nanoindentation system. *Thin Solid Films* **290–291**, 348 (1996).
8. N.X. Randall, C. Julia-Schmutz, J.M. Soro, J. von Stebut, and G. Zacharie: Novel nanoindentation method for characterizing multiphase materials. *Thin Solid Films* **308–309**, 297 (1997).
9. F. Wang and X. Kewei: An investigation of nanoindentation creep in polycrystalline Cu thin film. *Mater. Lett.* **58**, 2345 (2004).
10. J. Woigard, B. Bellaton, and R. Consiglio: U.S. Patent No. WO 2006/069847 A1, July 6, 2006.
11. A. C. Fischer-Cripps: *Nanoindentation* (Springer-Verlag), p. 198.
12. A.C. Fischer-Cripps, P. Karvankova, and S. Veprek: On the measurement of hardness of super-hard coatings. *Surf. Coat. Technol.* **200**, 5645 (2006).
13. W.C. Oliver and G.M. Pharr: Measurement of hardness and elastic modulus by instrumented indentation: Advances in understanding and refinements to methodology. *J. Mater. Res.* **19**(1), 3 (2004).
14. B.N. Lucas, W.C. Oliver, G.M. Pharr, and J-L. Loubet: Time dependent deformation during indentation testing, in *Thin Films: Stresses and Mechanical Properties VI*, edited by W.W. Gerberich, H. Gao, J-E. Sundgren, and S.P. Baker (Mater. Res. Soc. Symp. Proc. **436**, Pittsburgh, PA, 1997), p. 233.
15. J. Chen and S.J. Bull: Assessment of the toughness of thin coatings using nanoindentation under displacement control. *Thin Solid Films* **494**, 1 (2006).
16. T.F. Page, W.C. Oliver, and C.J. McHargue: The deformation behavior of ceramic crystals subjected to very low load (nano) indentations. *J. Mater. Res.* **7**(2), 450 (1992).
17. W.C. Oliver and G.M. Pharr: An improved technique for determining hardness and elastic modulus using load and displacement sensing indentation experiments. *J. Mater. Res.* **7**(6), 1564 (1992).
18. K. Van Vliet, L. Prchlik, and J.F. Smith: Direct measurement of indentation frame compliance. *J. Mater. Res.* **19**(1), 325 (2004).
19. C.A. Tweedie and K. Van Vliet: Contact creep compliance of viscoelastic materials via nanoindentation. *J. Mater. Res.* **21**(6), 1576 (2006).
20. G. Feng and A.H.W. Ngan: Effects of creep and thermal drift on modulus measurement using depth-sensing indentation. *J. Mater. Res.* **17**(3), 660 (2002).
21. D. Beegan, S. Chowdhury, and M.T. Laugier: The nanoindentation behaviour of hard and soft films on silicon substrates. *Thin Solid Films* **466**, 167 (2004).